Desalination and Water Treatment
www.deswater.com
doi: 10.1080/19443994.2014.943469

53 (2015) 1471–1481
February

Taylor & Francis
Taylor & Francis Group

Model for predicting transmembrane pressure jump for various membrane bioreactors

Hiromasa Kaneko, Kimito Funatsu*

Department of Chemical System Engineering, The University of Tokyo, Hongo 7-3-1, Bunkyo-ku, Tokyo 113-8656, Japan, Tel. +81 3 5841 8837; Fax: +81 3 5841 7771; email: hkaneko@chemsys.t.u-tokyo.ac.jp (H. Kaneko), Tel. +81 3 5841 7751; Fax: +81 3 5841 7771; email: funatsu@chemsys.t.u-tokyo.ac.jp (K. Funatsu)

Received 2 October 2013; Accepted 5 December 2013

ABSTRACT

Membrane bioreactors (MBRs) are widely used to purify wastewater for reuse. One crucial problem is membrane fouling. To reduce membrane fouling, chemical cleaning must be performed because some foulants cannot be removed by physical cleaning and these foulants will prevent the recovery of membrane performance. Hence, to allow chemical cleaning at an appropriate time, membrane fouling must be predicted in the long term. When an MBR plant is operated under a condition of constant-rate filtration, this corresponds to prediction of the transmembrane pressure (TMP). Because one reason to make TMP difficult to predict is a TMP jump, we have been developing a model that predicts the time of a TMP jump. In this study, many data-sets measured in MBRs that differ in operating conditions, such as flux and reactor size, and water quality, such as viscosity and mixed liquor suspended solids concentration, were collected from the literature. Then, TMP jump prediction models having high prediction performance could be constructed for each type and each material of membrane. In addition, we discussed MBR parameters, such as reactor volume and aeration that would be important for TMP jump prediction and membrane fouling.

Keywords: Membrane bioreactor; Fouling; Transmembrane pressure jump; Prediction

1. Introduction

Membrane bioreactors (MBRs) have been widely used in water treatment fields, such as sewage treatment and industrial wastewater treatment, to purify wastewater for reuse [1]. MBRs combine biological treatment with membrane filtration. First, bacteria within activated sludge metabolize the organic pollutants and produce environmentally acceptable metabolites, then a microfiltration or ultrafiltration membrane separates liquids from solids. MBR can be distributed at various locations such as residential sections and industrial plants. Thus, we can create an environment in which treated water is effectively reused in society.

However, MBRs have some practical problems. One of the critical problems is membrane fouling [2]. Membrane fouling is a phenomenon wherein foulants, such as activated sludge, sparingly soluble compounds, and high-molecular-weight solutes and

*Corresponding author.

Presented at the conference Engineering with Membranes – Towards a Sustainable Future (EWM 2013) Saint-Pierre d'Oléron, France, 3–7 September 2013

colloids, absorb or deposit on the membrane surface and absorb into and block the membrane pores. For example, in cases where the MBR is operated under constant-rate filtration, much energy is required to achieve a constant permeate flow rate owing to membrane fouling. To reduce membrane fouling, physical cleaning and chemical cleaning must be carried out with chemical reagents after a given period of processing time, when the transmembrane pressure (TMP) exceeds a given value, because some foulants cannot be removed by physical cleaning such as aeration, backwashing, or back pulsing, and these residual foulants will prevent the recovery of membrane performance. Frequent chemical cleaning and replacement of membranes are both expensive.

Hence, to allow chemical cleaning at an appropriate time, membrane fouling must be predicted in the long term [3–8]. When an MBR plant is operated under a condition of constant-rate filtration, this corresponds to prediction of the TMP [9–17]. Moreover, for MBR systems to be used widely as mentioned above, each MBR must be able to be operated automatically and controlled remotely. The TMP must be predicted *a priori* and a schedule of chemical cleaning must be created in advance, because a certain amount of time, for example, one week, is required for preparation of the chemicals for chemical cleaning. In addition, when distributed MBR systems are operated, it is difficult to check each MBR manually and we must make a schedule of chemical cleaning and prepare for chemical cleaning for each MBR beforehand.

One of the reasons to make TMP difficult to predict is a TMP jump [18]. After the long-term operation of MBR under the condition of constant-rate filtration, TMP increases rapidly [19]. This is called a TMP jump. Yu et al. proposed a mechanism for the TMP jump whereby the membrane is partially blocked by foulants, after which the local flux exceeds a critical flux [20], below which only reversible fouling happens and irreversible fouling can be neglected [21]. It can be said that a TMP jump is a rapid increase in TMP after a period of processing even though the measured flux is less than the critical flux.

We proposed the construction of a model that predicts the time of a TMP jump previously [22], which is based on the concept of critical flux [20] and statistical methods. The model where input variables $\boldsymbol{X}$ are time, flux, TMP and other MBR parameters such as operating conditions (aeration rate, hydraulic retention time (HRT), sludge retention time (SRT), and so on), and water quality (water temperature, total organic carbon, concentrations of extracellular polymeric substances (EPS) and soluble microbial products (SMP), and so on), and an output variable $\boldsymbol{y}$ is a label variable representing whether TMP jumps happen or not is constructed by using physical and statistical approaches. The model used to detect a TMP jump is called as a discriminant model. This model f is represented as $\boldsymbol{y} = f(\boldsymbol{X})$ and constructed with data of $\boldsymbol{X}$ measured in MBRs and those of $\boldsymbol{y}$ where the presence of TMP jumps is labeled. A support vector machine (SVM) [23], which is a nonlinear classification method, was applied for the construction of f. By inputting new data of $\boldsymbol{X}$ into f, we can estimate whether a TMP jump happens or not at the time when the new data are measured. Also, the presence of a TMP jump can be predicted at the target time by inputting setting values into f. In addition, the domains, where a discriminant model estimates TMP jumps happen, can be visualized to discuss the possibility of TMP jumps and the ways to prevent TMP jumps in the future [24].

However, each discriminant model must be constructed for each MBR, i.e. a discriminant model constructed with data measured in an MBR cannot be applied to other MBRs. In this study, therefore, we construct discriminant models that can be used for various types of MBR plants. First, from the literature, we collect many data-sets measured in MBRs that differ in operating conditions such as flux, HRT, SRT, and reactor size, and water quality such as viscosity and mixed liquor suspended solids (MLSS) concentration. Second, discriminant models are constructed for each type and each material of membrane because the interactions between foulants and membrane are different in each type and each material of membrane [25]. The type means flat membrane and hollow fiber membrane, and the material means polyvinylidene (PVDF), polyethylene (PE), polyethersulfone (PES), and so on.

In addition, we discuss MBR parameters that are important for TMP jump prediction and membrane fouling. The relationships between membrane fouling and MBR parameters, such as flux [26], SRT [27], temperature [28–31], MLSS [32,33], EPS [32–34], SMP [35], and F/M [36], have been investigated by many groups. Though some MBR parameters cannot be included in input variables of discriminant models when those parameters are not measured in many papers, we check the effect of as many parameters as possible to the performance of the discriminant models, as long as several data-sets remain.

2. Method

To predict the time of TMP jumps, a nonlinear function was derivated, based on Darcy's law, the relationship between flux and flow rate, resistance-in-series model, parallel resistance model and the equation of cake fouling [22]. The details of derivation of a nonlinear function for predicting the presence or absence of TMP jumps are shown in Appendix A. However, the derivated function is difficult and impractical to solve. Therefore, the function judging whether TMP jumps will happen or not is solved statistically using various data-sets measured in many MBRs. The basic concept of the TMP jump discriminant model is shown in Fig. 1. Input variables $\boldsymbol{X}$ are time, flux, TMP, and other MBR parameters, and an output variable $\boldsymbol{y}$ is a label variable representing whether there are TMP jumps. The data before TMP jumps are labeled –1, the data after TMP jumps are labeled 1, and an SVM model determining values of –1, and 1 is then constructed for $\boldsymbol{X}$ and $\boldsymbol{y}$. The details of SVM are shown in Appendix B.

Fig. 2 shows image of the actual use of the TMP jump discriminant model. In the prediction of a TMP jump in the long term, the target time is input, a set flux relating to the constant-rate filtration is entered, and the predicted TMP should be entered into the SVM model. The TMP values are predicted with Eqs. (A1) and (A4) in Appendix A. Fortunately, the increase in TMP is represented as a linear function of time because the initial increase in the fouling resistance can be assumed to be due to cake fouling. Predicted TMP values are then entered into the discriminant model. For other parameters, predicted values or set values are entered into the model. Accordingly, we can predict whether a TMP jump will happen at target time.

Using the constructed discriminant model and inputting future set values of flux and water quality with changing them, i.e. repeating trial and error, we can search the conditions where a TMP jump will hardly happen. MBR can be accordingly controlled for a TMP jump not to happen in the future. In addition, by projecting the results of a discriminant model to a two-dimensional map with visualization methods such as principal component analysis [37], kernel PCA [38], self-organizing map [39], and generative topographic mapping [40], we can discuss optimal MBR conditions where TMP jumps hardly happen [24].

3. Results and discussion

We analyzed discriminant models using operating data measured in various MBRs. The data-sets were collected from the literature. The types of membrane are flat membrane and hollow fiber membrane, and the materials of membrane are PVDF, PE, and PES. Table 1 shows the numbers of papers from which MBR data were collected and batches for each type and each material of membrane. A batch of data means the operation from the start or membrane fouling to next membrane cleaning or the end of operation. Quality and quantity of raw water and operating conditions are varied by MBRs.

To determine $\boldsymbol{y}$ in Fig. 1, we defined the data before TMP jumps (–1) and the data after the TMP jumps (1). First, a straight line approximating TMP by time was constructed with the first some data. The data whose absolute error of the approximation was less 2 kPa were labeled as −1, and the data whose absolute error of the approximation was equal to or more than 2 kPa were labeled as 1. The detailed process should be referred to the papers [22].

Table 2 shows the input variables for each type and each material of membrane. Time, flux, and TMP are included in all types and materials of membrane. However, other variables representing operating conditions and water quality are different in types and materials of membrane because there is no information on an MBR parameter for some papers.

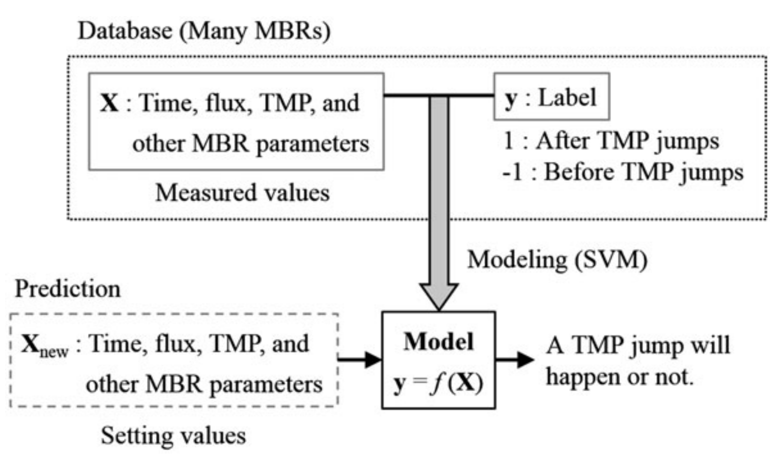

Fig. 1. TMP jump discriminant model.

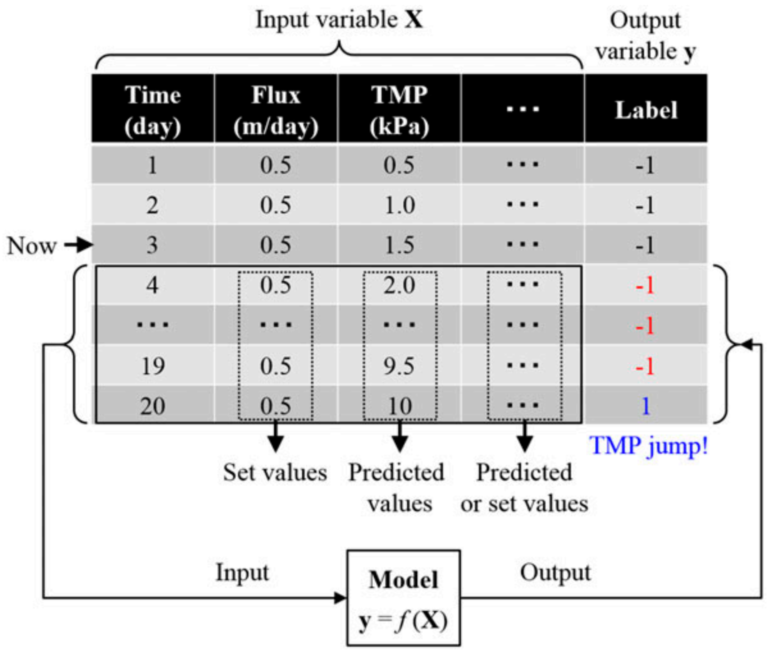

Fig. 2. Image of the actual use of the TMP jump discriminant model.

Table 1
The number of papers and batches that are collected for the analysis of TMP jump discriminant models in this paper

Type	Flat membrane			Hollow fiber membrane	
Material	PVDF	PE	PES	PVDF	PE
The number of papers	13 [41–53]	2 [54,55]	3 [56–58]	7 [59–65]	14 [58,59,66–77]
The number of batches	26	5	6	13	22

Table 2
The input variables for each type and each material of membrane

Type	Material	The number of input variables	Input variables
Flatmembrane	PVDF	11	Time, flux, TMP, MBR type (2), filtration mode (2), tank type for membrane (3), and viscosity
	PE	7	Time, flux, TMP, MBR type (2), reactor volume, and mixed liquor suspended solids (MLSS)
	PES	7	Time, flux, TMP, MBR type (2), pore size, and reactor volume
Hollow fiber membrane	PVDF	7	Time, flux, TMP, MBR type (2), pore size, and viscosity
	PE	7	Time, 1/V, TMP, MBR type (2), and tank type for membrane (2)

The discriminant models were constructed with the data-set of each type and each material of membrane for the accurate prediction of TMP jumps. Table 3 shows the results of construction of discriminant models. The accuracy rate (AR), precision (PR), and the detection rate (DR) are defined as follows [Eqs. (1)–(3)]:

$$\mathrm{AR} = \frac{\mathrm{TP} + \mathrm{TN}}{\mathrm{TP} + \mathrm{FP} + \mathrm{TN} + \mathrm{FN}} \quad (1)$$

$$\mathrm{PR} = \frac{\mathrm{TP}}{\mathrm{TP} + \mathrm{FP}} \quad (2)$$

Table 3
Modeling and prediction results

	Flat membrane			Hollow fiber membrane	
	PVDF	PE	PES	PVDF	PE
AR [%]	95.6	99.9	93.5	90.4	91.6
PR [%]	94.2	100	90.1	97.5	99.4
DR [%]	94.6	99.6	97.3	85.5	73.8
AR_{CV} [%]	94.4	99.4	83.0	91.2	88.0
PR_{CV} [%]	92.3	97.0	75.8	88.1	88.2
DR_{CV} [%]	93.7	99.6	96.0	97.9	71.4

$$DR = \frac{TP}{TP + FN} \tag{3}$$

Here, TP denotes the number of true positives, i.e. the number of samples for which the state after TMP jumps is correctly detected; TN represents the number of true negatives, i.e. the number of samples for which the state after TMP jumps is not detected and the transition is, indeed, incomplete; FP denotes the number of false positives, i.e. the number of samples for which the state after TMP jumps is incorrectly detected; and FN represents the number of false negatives, i.e. the number of samples for which TMP jumps is actually complete but it is not detected. AR_{CV}, PR_{CV}, and DR_{CV} are the AR, PR, and DR calculated by using cross-validation based on batches. First, the original data are divided into batches. Then, one batch is used as the data for validating the model constructed using the data of the other batches. This procedure is repeated so that each batch is used once as the validation data. Finally, not calculated but predicted values of $\mathbf{y}$ can be obtained. Therefore, AR_{CV}, PR_{CV}, and DR_{CV}, which are obtained by this cross-validation, mean the predictive ability of the constructed model, while AR, PR, and DR mean the accuracy of the model.

From Table 3, the discriminant models having high AR, PR, and DR values of more than 90% could be constructed for flat membrane. We achieved highly accurate discriminant models. In addition, AR_{CV}, PR_{CV}, and DR_{CV} that are indexes of the predictive performance indicated over 90% for flat membrane of PVDF and PE, and over 85% for hollow fiber membrane of PVDF. It was confirmed that some discriminant models can predict TMP jumps appropriately even in inputting data measured in MBRs different from the MBRs that are used for the model construction into the discriminant model if the same type and the same material of membrane are used.

Fig. 3 shows the plots of actual and predicted time of TMP jump. The unit of time is the second. From Fig. 3(a), one point is far from the diagonal, which

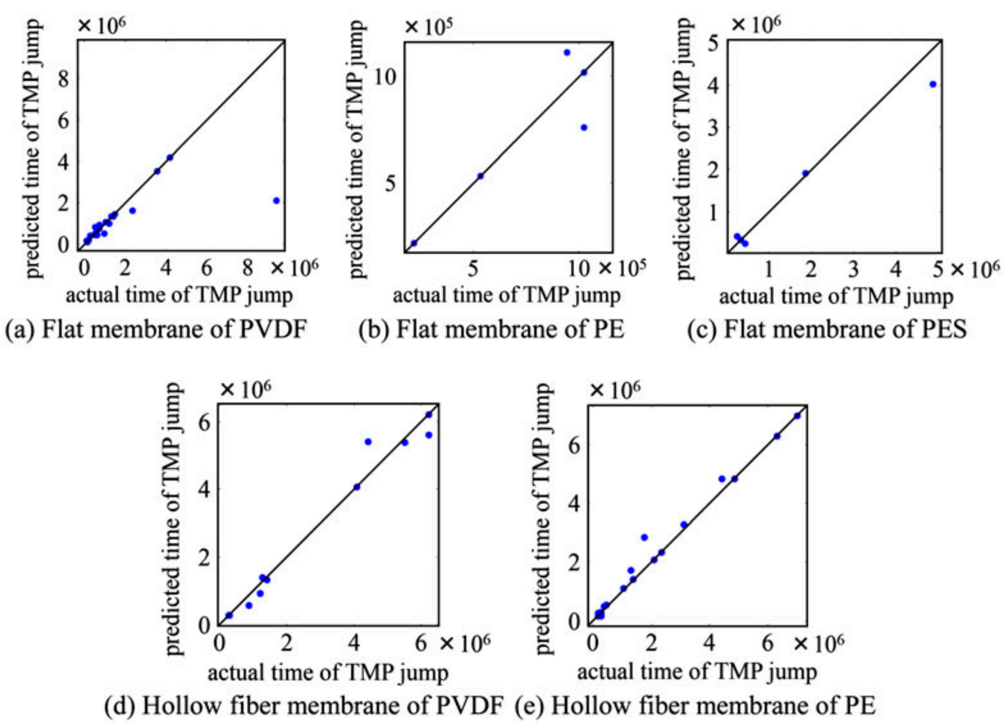

Fig. 3. The plots of actual and predicted time of TMP jump. The unit of time is the second.

means the prediction was failed. This would be because only one datum of time of the TMP jump exceeded 9×10^6 s and the TMP jump discriminant model constructed with the other data could not predict the time of the TMP jump of the datum, which was completely different from the other data. Applicability domain [78–80] of the constructed model must be considered in practice. On the other hand, most data in Fig. 3 are close to the diagonal, reflecting that the TMP jump discriminant models can predict the time of TMP jumps correctly.

Examples of TMP jump prediction results of flat membrane of PVDF and PE, and hollow fiber membrane of PVDF are shown in Fig. 4. The four batches in Fig. 4 came from the different papers. Although the time scale and the TMP scale are different in Fig. 4(a) and (b), the discriminant model could predict the times of TMP jumps accurately. The TMP jump discriminant models can be applied to MBRs other than the MBRs where training data are measured and can be used to discuss optimal MBR systems where TMP jumps hardly happen.

However, the PR_{CV} value in the cross-validation is not so high in the case of flat membrane of PES and the DR_{CV} value in cross-validation is not so high as well in the case of hollow fiber membrane of PE (see Table 3). For the case of flat membrane of PES, the number of batches is small in Table 1, and then, we focused on the case of hollow fiber membrane of PE in this paper. To increase predictive performance of the TMP jump discriminant model, other MBR parameters should be added to the input variables. However, an MBR parameter is not measured or described in all papers on hollow fiber membrane of PE. The addition of a new input variable means the decrease of batches or data-sets. Hence, we added new MBR parameters to the input variables one by one. Table 4 shows the additional input variables. These parameters were selected so that the number of batches was as large as possible.

Table 5 shows the modeling and prediction results when each MBR parameter is added to the seven input variables shown in Table 2 for hollow fiber membrane of PE. For A: pore size, and B: viscosity; the number of batches did not decrease so much, but the DR_{CV} value remained small. On the other hand, the DR_{CV} value greatly increased by adding C: reactor volume, D: HRT, or E: aeration, and especially the

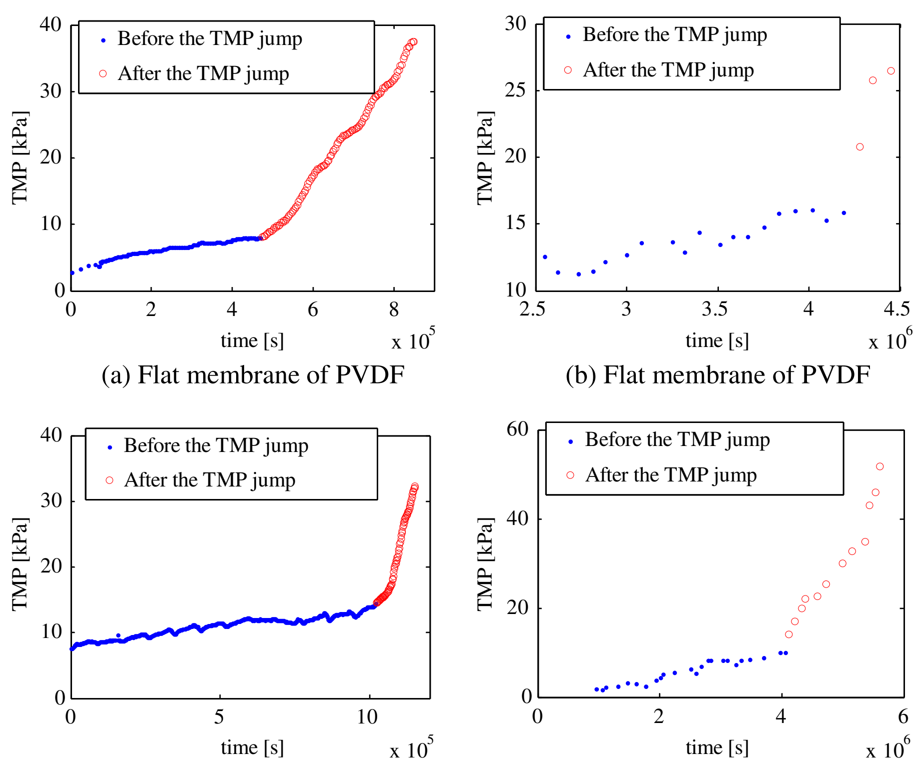

(a) Flat membrane of PVDF
(b) Flat membrane of PVDF
(c) Flat membrane of PE
(d) Hollow fiber membrane of PVDF

Fig. 4. Examples of prediction results.

Table 4
The additional input variables for hollow fiber membrane of PE

A	Pore size
B	Viscosity
C	Reactor volume
D	Hydraulic retention time
E	Aeration

Table 5
Modeling and prediction results for hollow fiber membrane of PE when each MBR parameter was added to the input variables. A, B, C, D, and E should be referred to Table 4

	A	B	C	D	E
The number of batches	21	21	16	14	14
AR [%]	92.1	90.9	95.5	95.5	96.1
PR [%]	98.0	94.6	92.3	99.1	99.1
DR [%]	75.5	76.3	94.7	86.6	90.0
AR_{CV} [%]	88.8	88.3	92.8	92.9	94.0
PR_{CV} [%]	93.7	87.1	96.9	95.6	92.2
DR_{CV} [%]	67.9	74.9	81.6	81.3	90.0

DR_{CV} value was 90.0% and the AR_{CV} and DR_{CV} values exceeded 90% when the discriminant model had aeration as an input variable. Although the number of batches were smaller than that of only seven input variables because there are no information on such MBR parameters in several papers, reactor volume, HRT, and aeration would be important for the prediction of TMP jumps and understanding MBR fouling.

To discuss the important variables for the prediction of TMP jumps, new MBR parameters were added to the input variables for flat sheet membrane of PVDF as is the case in hollow fiber membrane of PE. Table 6 shows the additional input variables for flat membrane of PVDF. A: pore size, B: HRT, and D: reactor volume are included also in Table 4. Table 7 shows the modeling and prediction results when each MBR parameter is added to the eleven input variables shown in Table 2 for flat membrane of PVDF. When A: pore size, B: HRT, C: SRT, or E: MLSS concentration was added to the input variables, the AR_{CV}, PR_{CV}, and DR_{CV} values were more than 90%. However, those values of D: reactor volume was lower than 90% and the predictive performance of the discriminant model decreased (see Tables 3 and 7). On the other hand, for hollow fiber membrane of PE, the predictive performance increased by adding reactor volume to the input variables (see Tables 3 and 5). This difference would be because the batches before the addition of reactor volume and the batches after the addition are different; the important input variables for the prediction of TMP jumps depend on the types and the materials of membrane; not one input variable but the combination of input variables relates TMP jumps and the relationships between reactor volume and other MBR parameters are considerable. The more data-sets and more information on MBR parameters are required to investigate the important variables and combinations of variables for TMP jumps and membrane fouling.

Table 6
The additional input variables for flat membrane of PVDF

A	Pore size
B	Hydraulic retention time
C	Sludge retention time
D	Reactor volume
E	MLSS concentration

Table 7
Modeling and prediction results for flat membrane of PVDF when each MBR parameter was added to the input variables. A, B, C, D, and E should be referred to Table 6

	A	B	C	D	E
The number of batches	23	20	19	17	14
AR [%]	96.0	95.4	96.0	90.8	96.0
PR [%]	94.8	94.7	94.9	94.6	98.5
DR [%]	95.0	93.5	94.9	87.9	94.1
AR_{CV} [%]	94.6	93.5	94.3	84.6	94.2
PR_{CV} [%]	92.1	90.9	91.4	83.5	97.4
DR_{CV} [%]	94.4	92.8	94.3	88.8	91.7

4. Conclusion

In this paper, we constructed discriminant models for predicting TMP jumps with MBR parameters. In the construction of the models, the operating data-sets measured in various MBRs were given in the literature. The high predictive accuracy of the models could be achieved for some types and some materials of membrane used in MBR plants. To increase the predictive performance for the model, whose AR_{CV}, PR_{CV}, and DR_{CV} values were low, we added several MBR parameters as the input variable one by one and checked the performance of the model. Then, reactor volume, HRT, and aeration would be important for the prediction of TMP jumps and understanding MBR fouling. However, reactor volume decreased the AR_{CV}, PR_{CV}, and DR_{CV} values in another type and material of membrane. The more data-sets and more information on MBR parameters are required to further investigate the important MBR parameters for TMP jumps and membrane fouling. When the important parameters can be found for a discriminant model, in the reference [24], the domains where a discriminant model estimates TMP jumps will happen is visualized. By visualizing the results of a discriminant model and analyzing set values of the MBR parameters using the visualization result, we can discuss the possibility of TMP jumps and the ways to prevent TMP jumps in the future.

By parameterizing the type and the material of membrane appropriately and using data-sets of various types and materials of membrane, the integrated discriminant model will be constructed with high prediction ability. To improve the performance of the discriminant models, the compressibility of cake appropriately. Using the TMP jump discriminant models, we will achieve the effective control of an MBR.

Acknowledgments

The authors acknowledge the support of the Core Research for Evolutional Science and Technology (CREST) project "Application of Integrated Intelligent Satellite System (IISS) to construct regional water resources utilization system" of the Japan Science and Technology Agency (JST). The authors also acknowledge the data collection of the MBR data for Ms Shoko Yashiro, Mr Tomonori Uchino and Mr Keiji Ito.

References

[1] F.G. Meng, S.R. Chae, A. Drews, M. Kraume, H.S. Shin, F.L. Yang, Recent advances in membrane bioreactors (MBRs): Membrane fouling and membrane material, Water Res. 43 (2009) 1489–1512.

[2] M. Kraume, D. Wedi, J. Schaller, V. Iversen, A. Drews, Fouling in MBR: What use are lab investigations for full scale operation? Desalination 236 (2009) 94–103.

[3] A. Broeckmann, J. Busch, T. Wintgens, W. Marquardt, Modeling of pore blocking and cake layer formation in membrane filtration for wastewater treatment, Desalination 189 (2006) 97–109.

[4] S. Jamal Khan, C. Visvanathan, V. Jegatheesanc, Prediction of membrane fouling in MBR systems using empirically estimated specific cake resistance, Bioresource Technol. 100 (2009) 6233–6136.

[5] J. Wu, C. He, X. Jiang, M. Zhang, Modeling of the submerged membrane bioreactor fouling by the combined pore constriction, pore blockage and cake formation mechanisms, Desalination 279 (2011) 127–134.

[6] M.K. Jørgensen, T.V. Bugge, M.L. Christensen, K. Keiding, Modeling approach to determine cake buildup and compression in a high-shear membrane bioreactor, J. Membr. Sci. 409–410 (2012) 335–345.

[7] T.V. Bugge, M.K. Jørgensen, M.L. Christensen, K. Keiding, Modeling cake buildup under TMP-step filtration in a membrane bioreactor: Cake compressibility is significant, Water Res. 46 (2012) 4330–4338.

[8] M. Park, J. Lee, C. Boo, S. Hong, S.A. Snyder, J.H. Kim, Modeling of colloidal fouling in forward osmosis membrane: Effects of reverse draw solution permeation, Desalination 314 (2013) 115–123.

[9] Y. Ye, V. Chen, A.G. Fane, Modeling long-term subcritical filtration of model EPS solutions, Desalination 191 (2006) 318–327.

[10] H. Monclúsa, G. Ferrero, G. Buttiglieri, J. Comas, I. Rodriguez-Roda, Online monitoring of membrane fouling in submerged MBRs, Desalination 277 (2011) 414–419.

[11] M.J. Kim, B. Sankararao, C.K. Yoo, Determination of MBR fouling and chemical cleaning interval using statistical methods applied on dynamic index data, J. Membr. Sci. 375 (2011) 345–353.

[12] M.J. Kim, G.Y. Yoo, C.K. Yoo, Development of combined fouling model in a membrane bioreactor, Asia-Pac. J. Chem. Eng. 6 (2011) 423–432.

[13] C.F. Galinha, G. Carvalho, C.A. Portugal, G. Guglielmi, M.A. Reis, JG Crespo, Multivariate statistically-based modelling of a membrane bioreactor for wastewater treatment using 2D fluorescence monitoring data, Water Res. 46 (2012) 3623–3636.

[14] H. Kaneko, K. Funatsu, A chemometric approach to prediction of transmembrane pressure in membrane bioreactors, Chemom. Intell. Lab. Syst. 126 (2013) 30–37.

[15] M.F.R. Zuthi, H.H. Ngo, W.S. Guo, J.X. Li, S.Q. Xia, Z.Q. Zhang, New proposed conceptual mathematical models for biomass viability and membrane fouling of membrane bioreactor, Bioresour. Technol. 142 (2013) 737–740.

[16] R.G.M. van der Sman, H.M. Vollebregt, Transient critical flux due to coupling of fouling mechanisms during crossflow microfiltration of beer, J. Membr. Sci. 435 (2013) 21–37.

[17] A. Robles, M.V. Ruano, J. Ribes, A. Seco, J. Ferrer, Mathematical modelling of filtration in submerged anaerobic MBRs (SAnMBRs): Long-term validation, J. Membr. Sci. 446 (2013) 303–309.

[18] G. Guglielmi, D. Chiarani, S.J. Judd, G. Andreottola, Flux criticality and sustainability in a hollow fibre submerged membrane bioreactor for municipal wastewater treatment, J. Membr. Sci. 229 (2004) 171–177.

[19] B.D. Cho, A.G. Fane, Fouling transients in nominally sub-critical flux operation of a membrane bioreactor, J. Membr. Sci. 209 (2002) 391–403.

[20] K.C. Yu, X.H. Wen, Q.J. Bu, H. Xia, Critical flux enhancements with air sparging in axial hollow fibers cross-flow microfiltration of biologically treated wastewater, J. Membr. Sci. 224 (2003) 69–79.

[21] P. Bacchin, P. Aimar, R.W. Field, Critical and sustainable fluxes: Theory, experiments and applications, J. Membr. Sci. 281 (2006) 42–69.
[22] H. Kaneko, K. Funatsu, Physical and statistical model for predicting a transmembrane pressure jump for a membrane bioreactor, Chemom. Intell. Lab. Syst. 121 (2013) 66–74.
[23] V.N. Vapnik, The nature of statistical learning theory, Springer, New York, NY, 1999.
[24] H. Kaneko, K. Funatsu, Visualization of models predicting transmembrane pressure jump for membrane bioreactor, Ind. Eng. Chem. Res. 51 (2012) 9679–9686.
[25] H. Lin, W. Peng, M. Zhang, J. Chen, H. Hong, Y. Zhang, A review on anaerobic membrane bioreactors: Applications, membrane fouling and future perspectives, Desalination 314 (2013) 169–188.
[26] M.A.H. Johir, J. George, S. Vigneswaran, J. Kandasamy, A. Sathasivan, A. Grasmick, Effect of imposed flux on fouling behavior in high rate membrane bioreactor, Bioresour. Technol. 122 (2012) 42–49.
[27] R.V.D. Broeck, J.V. Dierdonck, P. Nijskens, C. Dotremont, P. Krzeminski, J.H.J.M. van der Graaf, J.B. van Lier, J.F.M.V. Impe, I.Y. Smets, The influence of solids retention time on activated sludge bioflocculation and membrane fouling in a membrane bioreactor (MBR), J. Membr. Sci. 401–402 (2012) 48–55.
[28] P. van den Brink, O.A. Satpradit, A. van Bentem, A. Zwijnenburg, H. Temmink, M. van Loosdrecht, Effect of temperature shocks on membrane fouling in membrane bioreactors, Water Res. 45 (2011) 4491–4500.
[29] W.J. Gao, X. Qu, K.T. Leung, B.Q. Liao, Influence of temperature and temperature shock on sludge properties, cake layer structure, and membrane fouling in a submerged anaerobic membrane bioreactor, J. Membr. Sci. 421–422 (2011) 131–144.
[30] C. Ma, S. Yu, W. Shi, SGJ Heijman, L.C. Rietveld, Effect of different temperatures on performance and membrane fouling in high concentration PAC–MBR system treating micro-polluted surface water, Bioresour. Technol. 141 (2013) 19–24.
[31] D.W. Gao, Z.D. Wen, B. Li, H. Liang, Membrane fouling related to microbial community and extracellular polymeric substances at different temperatures, Bioresour. Technol. 143 (2013) 172–177.
[32] F. Meng, H. Zhang, F. Yang, S. Zhang, Y. Li, X. Zhang, Identification of activated sludge properties affecting membrane fouling in submerged membrane bioreactors, Sep. Purif. Technol. 51 (2006) 95–103.
[33] Y.J. Liu, D.D. Sun, Membrane fouling mechanism in dead-end microfiltration of denitrifying granular sludge mixed liquors developed in SBRs at different calcium concentrations, J. Membr. Sci. 396 (2012) 74–82.
[34] J. Li, X. Zhang, F. Cheng, Y. Liu, New insights into membrane fouling in submerged MBR under sub-critical flux condition, Bioresour. Technol. 137 (2013) 404–408.
[35] Z. Geng, E.R. Hall, P.R. Bérubé, Membrane fouling mechanisms of a membrane enhanced biological phosphorus removal process, J. Membr. Sci. 296 (2007) 93–101.
[36] Y. Liu, H. Liu, L. Cui, K. Zhang, The ratio of food-to-microorganism (F/M) on membrane fouling of anaerobic membrane bioreactors treating low-strength wastewater, Desalination 297 (2012) 97–103.
[37] S. Wold, K. Esbensen, P. Geladi, Principal component analysis, Chemom. Intell. Lab. Syst. 2 (1987) 37–52.
[38] K.R. Muller, S. Mika, G. Ratsch, K. Tsuda, B. Scholkopf, An introduction to kernel-based learning algorithms, IEEE Trans. Neural Networks 12 (2001) 181–201.
[39] T. Kohonen, The self-organizing map, Proc. IEEE 78 (1990) 1464–1480.
[40] C.M. Bishop, M. Svensen, C.K.I. Williams, GTM: The generative topographic mapping, Neural Comput. 10 (1998) 215–234.
[41] J. Phattaranawik, T. Leiknes, Study of hybrid vertical anaerobic sludge-aerobic biofilm membrane bioreactor for wastewater treatment, Water Environ. Res. 82 (2010) 273–280.
[42] K. Xie, H.J. Lin, B. Mahendran, D.M. Bagley, K.T. Leung, Performance and fouling characteristics of a submerged anaerobic membrane bioreactor for kraft evaporator condensate treatment, Environ Technol. 31 (2010) 511–521.
[43] A. Grélot, P. Grelier, A. Tazi-Pain, B. Lesjean, U. Brüss, A. Grasmick, B. Lesjean, U. Bruss, A. Grasmick, Performances and fouling control of a flat sheet membrane in a MBR pilot-plant, Water Sci. Technol. 61 (2010) 2185–2192.
[44] Z.W. Wang, S.J. Tang, Y.F. Zhu, Z.C. Wu, Q. Zhou, D.H. Yang, Fluorescent dissolved organic matter variations in a submerged membrane bioreactor under different sludge retention times, J. Membr. Sci. 355 (2010) 151–157.
[45] H.J. Lin, K. Xie, B. Mahendran, D.M. Bagley, K.T. Leung, S.N. Liss, B.Q. Liao, Factors affecting sludge cake formation in a submerged anaerobic membrane bioreactor, J. Membr. Sci. 361 (2010) 126–134.
[46] X.F. Li, L.N. Zhang, G.C. Du, Influence of sludge discharge on sludge settleability and membrane flux in a membrane bioreactor, Environ Technol. 11 (2010) 1289–1294.
[47] Z.C. Wu, Q.Y. Wang, Z.W. Wang, Y.Q. Ma, Q. Zhou, D.H. Yang, Membrane fouling properties under different filtration modes in a submerged membrane bioreactor, Process Biochem. 45 (2010) 1699–1706.
[48] A. Sweity, W. Ying, M.S. Ali-Shtayeh, F. Yang, A. Bick, G. Oron, M. Herzberg, Relation between EPS adherence, viscoelastic properties, and MBR operation: Biofouling study with QCM-D, Water Res. 45 (2011) 6430–6440.
[49] K. Chen, X. Wang, X. Li, J. Qian, X. Xiao, Impacts of sludge retention time on the performance of submerged membrane bioreactor with the addition of calcium ion, Sep. Purif. Technol. 82 (2011) 148–155.
[50] X.L. Yang, H.L. Song, M. Chen, B. Cheng, Characterizing membrane foulants in MBR with addition of polyferric chloride to enhance phosphorus removal, Bioresource Technol. 102 (2011) 9490–9496.
[51] H. Lin, F. Wang, L. Ding, H. Hong, J. Chen, X. Lu, Enhanced performance of a submerged membrane bioreactor with powdered activated carbon addition for municipal secondary effluent treatment, J. Hazard. Mater. 192 (2011) 1509–1514.
[52] Q. Wang, Z. Wang, Z. Wu, X. Han, Sludge reduction and process performance in a submerged membrane bioreactor with aquatic worms, Chem. Eng. J. 172 (2011) 929–935.

[53] K.K. Ng, C.F. Lin, S.C. Panchangam, P.K.A. Hong, P.Y. Yang, Reduced membrane fouling in a novel bio-entrapped membrane reactor for treatment of food and beverage processing wastewater, Water Res. 45 (2011) 4269–4278.

[54] X.M. Wang, X.Y. Li, Accumulation of biopolymer clusters in a submerged membrane bioreactor and its effect on membrane fouling, Water Res. 42 (2008) 855–862.

[55] G. Guglielmi, D. Chiarani, D.P. Saroj, G. Andreottola, Impact of chemical cleaning and air-sparging on the critical and sustainable flux in a flat sheet membrane bioreactor for municipal wastewater treatment, Water Sci. Technol. 57 (2008) 1873–1879.

[56] Z. Wang, Z. Wu, S. Tang, Impact of temperature seasonal change on sludge characteristics and membrane fouling in a submerged membrane bioreactor, Sep. Purif. Technol. 45 (2010) 920–927.

[57] Z.W. Wang, Z.C. Wu, G.P. Yu, H.F. Liu, Z. Zhou, Relationship between sludge characteristics and membrane flux determination in submerged membrane bioreactors, J. Membr. Sci. 284 (2006) 87–94.

[58] S.J. Khan, C. Visvanathan, Influence of mechanical mixing intensity on a biofilm structure and permeability in a membrane bioreactor, Desalination 231 (2008) 253–267.

[59] N. Yamato, K. Kimura, T. Miyoshi, Y. Watanabe, Difference in membrane fouling in membrane bioreactors (MBRs) caused by membrane polymer materials, J. Membr. Sci. 280 (2006) 911–919.

[60] Q. Liu, X.C. Wang, Y. Liu, H. Yuan, Y. Du, Performance of a hybrid membrane bioreactor in municipal wastewater treatment, Desalination 258 (2010) 143–147.

[61] K. Ouyang, J.X. Liu, Effect of sludge retention time on sludge characteristics and membrane fouling of membrane, J. Environ. Sci. 21 (2009) 1329–1235.

[62] K. Kimura, T. Naruse, Y. Watanabe, Changes in characteristics of soluble microbial products in membrane bioreactors associated with different solid retention times: Relation to membrane fouling, Water Res. 43 (2009) 1033–1039.

[63] H.F. Zhang, B.S. Sun, X.H. Zhao, Z.H. Gao, Effect of ferric chloride on fouling in membrane bioreactor, Sep. Purif. Technol. 63 (2008) 341–347.

[64] L.M. Yuan, C.Y. Zhang, Y.Q. Zhang, Y. Ding, D.L. Xi, Biological nutrient removal using an alternating of anoxic and anaerobic membrane bioreactor (AAAM) process, Desalination 221 (2008) 566–575.

[65] I. Ivanovic, T.O. Leiknes, Impact of the performance of a biofilm-MBR (BF-MBR), Desalination 283 (2011) 641–644.

[66] K. Sombatsompop, C. Visvanathan, R.B. Aim, Evaluation of biofouling phenomenon in suspended and attached growth membrane bioreactor systems, Desalination 201 (2006) 138–149.

[67] Q. Yang, J. Chen, F. Zhang, Membrane fouling control in a submerged membrane bioreactor with porous, flexible suspended carriers, Desalination 189 (2006) 292–302.

[68] N. Fallah, B. Bonakdarpour, B. Nasernejad, M.R.A. Moghadam, Long-term operation of submerged membrane bioreactor (MBR) for the treatment of synthetic wastewater containing styrene as volatile organic compound (VOC): Effect of hydraulic retention time (HRT), J. Hazard. Mater. 178 (2010) 718–724.

[69] Y. Watanabe, T. Itonaga, Hybrid municipal wastewater treatment system with pre-coagulation/sedimentation, J. Ind. Eng. Chem. 10 (2004) 122–128.

[70] T. Itonaga, K. Kimura, Y. Watanabe, Influence of suspension viscosity and colloidal particles on permeability of membrane used in membrane bioreactor (MBR), Water Sci. Technol. 50 (2004) 301–309.

[71] W.T. Zhao, X. Huang, D.J. Lee, X.H. Wang, Y.X. Shen, Use of submerged anaerobic-anoxic-oxic membrane bioreactor to treat highly toxic coke wastewater with complete sludge retention, J. Membr. Sci. 330 (2009) 57–64.

[72] X. Huang, J.L. Wu, Improvement of membrane filterability of the mixed liquor in a membrane bioreactor by ozonation, J. Membr. Sci. 318 (2008) 210–216.

[73] F.I. Hai, K. Yamamoto, K. Fukushi, Different fouling modes of submerged hollow-fiber and flat-sheet membranes induced by high strength wastewater with concurrent biofouling, Desalination 180 (2005) 89–97.

[74] J.L. Wu, X. Huang, Effect of dosing polymeric ferric sulfate on fouling characteristics, mixed liquor properties and performance in a long-term running membrane bioreactor, Sep. Purif. Technol. 63 (2008) 45–52.

[75] K. Kimura, N. Yamato, H. Yamamura, Y. Watanabe, Membrane fouling in pilot-scale membrane bioreactors (MBRs) treating municipal wastewater, Environ. Sci. Technol. 39 (2005) 6293–6299.

[76] S.H. Hong, W.N. Lee, H.S. Oh, K.M. Yeon, B.K. Hwang, C.H. Lee, I.S. Chang, S. Lee, The effects of intermittent aeration on the characteristics of bio-cake layers in a membrane bioreactor, Environ. Sci. Technol. 41 (2007) 6270–6276.

[77] M. Xu, X. Wen, Z. Yu, Y. Li, X. Huang, A hybrid anaerobic membrane bioreactor coupled with online ultrasonic equipment for digestion of waste activated sludge, Bioresource Technol. 102 (2011) 5617–5625.

[78] I. Sushko, S. Novotarskyi, R. Körner, A.K. Pandey, A. Cherkasov, J. Li, P. Gramatica, K. Hansen, T. Schroeter, K.R. Müller, L. Xi, H. Liu, X. Yao, T. Öberg, F. Hormozdiari, P. Dao, C. Sahinalp, R. Todeschini, P. Polishchuk, A. Artemenko, V. Kuz'min, T.M. Martin, D.M. Young, D. Fourches, E. Muratov, A. Tropsha, I. Baskin, D. Horvath, G. Marcou, C. Muller, A. Varnek, V.V. Prokopenko, I.V. Tetko, Applicability domains for classification problems: Benchmarking of distance to models for ames mutagenicity set, J. Chem. Inf. Model. 50 (2010) 2094–2111.

[79] I.I. Baskin, N. Kireeva, A. Varnek, The one-class classification approach to data description and to models applicability domain, Mol. Inf. 29 (2010) 581–587.

[80] H. Kaneko, K. Funatsu, Estimation of predictive accuracy of soft sensor models based on data density, Chemom. Intell. Lab. Syst. 128 (2013) 111–117.

[81] D. Sperry, F. Baker, Notes and correspondence: A study of the fundamental laws of filtration using plant-scale equipment, Ind. Eng. Chem. 13 (1921) 1163–1165.

[82] C.C. Chang, C.J. Lin, LIBSVM: A library for support vector machines, 2001. Available from: http://www.csie.ntu.edu.tw/~cjlin/libsvm.

Appendix A. Derivation of a nonlinear function for predicting the presence or absence of TMP jumps [22]

Viscosity, μ; transmembrane flux, J; and total filtration resistance, R, have the following Eq. (A1)

$$TMP_t = \mu_t J_t R_t \tag{A1}$$

where t is the time and these variables are functions of time. This equation is called Darcy's law. The resistance-in-series model of R is represented as follows [Eq. (A2)]:

$$R_t = R_m + R_{f,t} + R_{other,t} \tag{A2}$$

where R_m is the intrinsic membrane resistance; R_f is the fouling resistance; and R_{other} is the other resistance due to water quality, such as EPS and SMP, in MBRs. R_f and R_{other} are functions of t. If cake filtration is assumed, the parallel resistance model of R_f is given as follows [Eq. (A3)]:

$$R_{f,t} = \frac{A_0}{A_t} R_{c,t} \tag{A3}$$

where A_0 is the total membrane area; A_t is the usable membrane area that is not blocked at time t; and R_c is the resistance due to cake fouling. When MBR is operated under constant-rate filtration, R_c is given as follows [Eq. (A4)]:

$$R_{c,t} = at + b \tag{A4}$$

where a and b are constant values. Though R_c is a exponential function of t, considering the compressibility of the filter cake [81], the function of initial R_c before a TMP jump will be approximated by the linear function of t like Eq. (A4).

J in Eq. (A1) is represented with treatment flow rate, V, as follows [Eq. (A5)]:

$$J_t = \frac{V_t}{A_t} \tag{A5}$$

The following Eq. (A6) is derived from Eqs. (A1)–(A5).

$$TMP_t = \mu_t \frac{V_t}{A_t}\left(R_m + \frac{A_0}{A_t}(at+b) + R_{other,t}\right) \tag{A6}$$

Then, if a mechanism of a critical flux, J_{crt}, proposed by Yu et al. [20] is adopted, a local flux exceeds J_{crt}. that is, the following [Eq. (A7)] meets, when a TMP jump happens.

$$J_t \geq J_{crt} \tag{A7}$$

Eqs. (A6) and (A7) are summarized as follows [Eq. (A8)]:

$$TMP_t - \mu J_{crt}\left(R_m + A_0(at+b)\frac{J_{crt}}{V_t} + R_{other,t}\right) \geq 0 \tag{A8}$$

Therefore, when the left-hand value of (A8) exceeds zero, a TMP jump happens. (A8) is a nonlinear function of t, TMP, V, and other MBR parameters such as operating conditions and water quality, which are assumed to relate μ, a, b, J_{crt}, and R_{other}. It is totally impractical to solve the function (A8) exactly and hence, this function is handled statistically. Input variables $\boldsymbol{X}$ are t, TMP, V (or flux J), and other MBR parameters such as operating conditions and water quality; the labels of data before TMP jumps are set as –1; the labels of data after TMP jumps are set as 1; and then, a model determining 1 or –1 is constructed by using a statistical method.

Appendix B. SVM [23]

For constructing an above discriminant model, an SVM method is used in this paper. An SVM is one of the classification methods used to generate nonlinear classifiers by applying the kernel approach. In a linear SVM, the discriminant function $f(\boldsymbol{x})$ is defined as follows [Eq. (B1)]:

$$f(\mathbf{x}) = \mathbf{x}\cdot\mathbf{w} + b \tag{B1}$$

where $\mathbf{x}$ is a query sample; $\mathbf{w}$ is a weight vector; and b is a bias. The primal form of the SVM can be expressed as an optimization problem:

Minimize [Eq. (B2)]

$$\frac{1}{2}\|\mathbf{w}\|^2 + C\sum_i \xi_i \tag{B2}$$

subject to [Eq. (B3)]

$$\begin{aligned} y_i(\mathbf{x}_i\cdot\mathbf{w} + b) &\geq 1 - \xi_i \\ y_i &\in \{-1, 1\} \end{aligned} \tag{B3}$$

where y_i and $\mathbf{x}_i$ represent training data; ξ_i is slack variables; and C is the penalizing factor that controls the trade-off between a training error and a margin. By minimizing (B2), we can construct a discriminant model that shows a good balance between the ability to adapt to the training data and the ability to generalize. In our application, a kernel function is a radial basis function as follows [Eq. (B4)]:

$$K(\mathbf{x},\mathbf{x}') = \exp\left(-\gamma\|\mathbf{x}-\mathbf{x}'\|^2\right) \tag{B4}$$

where γ is the tuning parameter that controls the width of the kernel function. Using (B.4), a nonlinear model can be constructed because the inner product of $\mathbf{x}$ and $\mathbf{w}$ in (B.1) is represented as the kernel function of $\mathbf{x}$. In this study, LIBSVM [82] is used as the machine learning software.